

# A Bench-to-Bioinformatics: Approach to Chamomile Oil Creams for the Treatment of Psoriasis

Umara Arif<sup>1</sup>, Zoya Abid<sup>2</sup>, Quratulain Aftab<sup>3</sup>, Rida Batool<sup>4</sup>, Faiza Mushtaq<sup>2</sup><sup>1</sup> MPhil Pharmacology, Faculty of Pharmaceutical & Allied Health Sciences, Lahore College for Women University, Lahore<sup>2</sup> MPhil Pharmaceutics, Khalid Mahmood Institute of Medical Sciences, Sialkot<sup>3</sup> Pharm-D, University of Sargodha; MPhil Pharmaceutics, Riphah International University<sup>4</sup> Pharm-D, MPhil in Pharmaceutical Chemistry, KIMS\*Corresponding author: Umara Arif, [umara.arif77@gmail.com](mailto:umara.arif77@gmail.com)**"Cite this Article"** Received: 17 January 2026; Accepted: 11 May 2026; Published: 06 June 2026**Author Contributions:** Author Contributions: Concept and study design: UA and ZA; formulation development and laboratory work: ZA, QA, and RB; data collection: UA, QA, RB, and FM; GC-MS, docking, and ADMET interpretation: RB and QA; animal-study supervision and pharmacological interpretation: UA and FM; statistical analysis and results interpretation: UA and ZA; manuscript drafting: UA, ZA, and QA; manuscript revision and final approval: UA, ZA, QA, RB, and FM. **Ethical Approval:** Lahore College for Women University, Lahore. **Informed Consent:** Written informed consent was obtained from all participants; **Conflict of Interest:** The authors declare no conflict of interest. **Funding:** No external funding; **Data Availability:** Available from the corresponding author on reasonable request; **Acknowledgments:** N/A.

## ABSTRACT

**Background:** Psoriasis is a chronic immune-mediated inflammatory skin disease characterized by abnormal keratinocyte proliferation, impaired epidermal differentiation, and recurrent scaly plaques. Chamomile oil contains bioactive constituents with reported anti-inflammatory and dermatological relevance, but its usefulness as a topical antipsoriatic candidate depends on stable formulation development, skin compatibility, release behavior, and preclinical biological activity. **Objective:** This study aimed to develop chamomile oil-based oil-in-water cream formulations at different concentrations and evaluate their physicochemical properties, stability, microbial quality, skin irritation potential, in vitro release behavior, mouse-tail antipsoriatic activity, histological effects, molecular docking profile, and ADMET characteristics. **Methods:** Chamomile oil was chemically profiled by GC-MS and incorporated into oil-in-water cream formulations coded C1, C2, C3, and C4, containing 1.25%, 2.5%, 5%, and 7.5% chamomile oil, respectively. The base cream without chamomile oil was coded C. Formulations were evaluated for organoleptic properties, pH, viscosity, spreadability, bleeding, loss on drying, accelerated stability, and microbial growth. Acute dermal irritation was assessed using an erythema and edema scoring system. Antipsoriatic activity was evaluated in an albino mouse-tail model using orthokeratosis and drug activity as outcome measures, with betamethasone as a reference comparator. The selected C3 formulation was further assessed using a modified Franz diffusion cell. Molecular docking was performed against psoriasis-related inflammatory targets, and ADMET prediction was conducted for the selected lead compound. **Results:** C1, C2, and C3 showed acceptable organoleptic and stability profiles, whereas C4 developed bleeding, phase separation, gritty texture, and instability and was excluded from mouse-tail efficacy testing. No microbial growth was reported after 24 hours. Drug activity increased with chamomile oil concentration, with C1, C2, and C3 showing 29.15%, 44.90%, and 61.12% activity, respectively, while betamethasone showed 66.38%. Histological findings supported improved granular layer formation and epidermal differentiation in treated groups, particularly with the 5% formulation. The Franz diffusion data for C3 showed decreasing reported percentage values from 67.35% at 15 minutes to 63.10% at 150 minutes and were therefore interpreted as time-specific calculated release estimates rather than confirmed cumulative release. Docking suggested predicted interactions of the lead compound with TNF- $\alpha$  and IL-17RA, while ADMET prediction showed favorable physicochemical features but a positive Ames toxicity prediction. **Conclusion:** The 5% chamomile oil cream showed the most favorable preclinical performance among the stable formulations, with drug activity numerically approaching the betamethasone comparator. The formulation demonstrated acceptable physicochemical characteristics, stability, and mouse-tail histological improvement under the tested conditions. However, release-method clarification, expanded toxicological evaluation, formulation optimization, larger controlled animal studies, and clinical validation are required before therapeutic application in humans. **Keywords:** Psoriasis; chamomile oil; oil-in-water cream; mouse-tail model; orthokeratosis; Franz diffusion cell; molecular docking; ADMET.

## INTRODUCTION

Psoriasis is a chronic, immune-mediated inflammatory skin disease characterized by abnormal keratinocyte proliferation, impaired epidermal differentiation, dermal and epidermal immune-cell infiltration, and recurrent erythematous scaly plaques. Although the disease is non-contagious, it imposes a considerable clinical and psychosocial burden because of pruritus, pain, visible lesions, cosmetic distress, and its association with systemic comorbidities such as psoriatic arthritis, cardiovascular disease, and metabolic syndrome (1). Current therapeutic options include topical corticosteroids, vitamin D analogues, systemic immunosuppressants, retinoids, phototherapy, and

biologic agents; however, long-term use may be limited by adverse effects, treatment cost, relapse after discontinuation, reduced adherence, and concerns regarding chronic steroid exposure in patients requiring repeated topical therapy (2). These limitations support continued investigation of affordable, locally acting, and formulation-optimized topical alternatives that may complement existing psoriasis management.

The pathogenesis of psoriasis involves a complex interaction between genetic predisposition, environmental triggers, innate immune activation, and adaptive immune dysregulation. Activated dendritic cells stimulate T-helper cell responses, particularly Th1, Th17, and Th22 pathways, leading to increased production of pro-inflammatory cytokines such as tumor necrosis factor-alpha (TNF- $\alpha$ ), interleukin-17 (IL-17), interleukin-22 (IL-22), and interferon-gamma (IFN- $\gamma$ ). These cytokines promote keratinocyte proliferation, suppress normal epidermal maturation, and sustain inflammatory feedback through nuclear factor kappa B (NF- $\kappa$ B)-associated signaling and other inflammatory cascades (3, 4). The resulting epidermal hyperplasia, parakeratosis, vascular alteration, and impaired granular layer formation are central histological features of psoriatic lesions. Therefore, topical agents with anti-inflammatory, antioxidant, antimicrobial, and keratinocyte-modulating potential may have relevance in preclinical psoriasis models, provided that their delivery system is stable, skin-compatible, and capable of supporting adequate local release.

Chamomile essential oil derived from *Matricaria chamomilla* has been investigated for anti-inflammatory, antioxidant, antimicrobial, and dermatological applications. Its pharmacological activity has been attributed to bioactive constituents such as  $\alpha$ -bisabolol, chamazulene,  $\alpha$ -pinene, flavonoids, and other terpenoid compounds, which may modulate inflammatory mediators through cyclooxygenase, lipoxygenase, cytokine-related, and NF- $\kappa$ B-associated pathways (5, 6). Experimental evidence also suggests that chamomile-based preparations may reduce inflammatory skin responses and support epidermal recovery in selected dermatological contexts (6). However, the therapeutic potential of chamomile oil in psoriasis cannot be inferred from phytochemical activity alone. Its usefulness as a topical candidate depends on formulation performance, physicochemical stability, skin compatibility, release behavior, and biological activity in a relevant preclinical model.

Oil-in-water cream systems are commonly used for topical dermatological delivery because they are generally acceptable to patients, easy to apply, cosmetically suitable, and capable of delivering lipophilic active constituents to the skin surface. For a topical antipsoriatic formulation, the active ingredient must be incorporated at a concentration that maintains physical stability while allowing sufficient local availability without irritation or phase separation. Physicochemical properties such as pH, viscosity, spreadability, homogeneity, bleeding tendency, loss on drying, microbial quality, and accelerated stability are therefore central to formulation acceptability and reproducibility (7). In vitro Franz diffusion cell testing provides a controlled method for studying release behavior from semisolid topical formulations and can help determine whether the active formulation releases measurable constituents over time under standardized experimental conditions (8). However, release data must be interpreted cautiously and should not be described as cumulative or sustained unless the calculation method and release profile support that interpretation.

The mouse-tail model remains a useful preclinical screening model for antipsoriatic activity because it allows histological assessment of orthokeratosis, granular layer formation, and epidermal differentiation. In this model, antipsoriatic activity is commonly inferred from the ability of a test formulation to promote conversion of parakeratotic regions toward orthokeratotic differentiation and to improve granular layer development (9). Although this model cannot reproduce the full immunological and systemic complexity of human psoriasis, it provides a practical experimental platform for comparing topical formulations, base cream, and reference treatments such as betamethasone. When combined with histopathological evaluation, irritation testing, in vitro release assessment, and

supportive in silico screening, it can provide preliminary preclinical evidence for selecting an optimized formulation for further investigation.

Despite the known anti-inflammatory potential of chamomile oil, limited integrated evidence is available on chamomile oil-based oil-in-water cream formulations evaluated across chemical profiling, physicochemical quality, stability, microbial assessment, skin irritation, Franz diffusion release testing, mouse-tail antipsoriatic activity, histology, molecular docking, and ADMET prediction within a single preclinical framework. The present study was therefore designed to formulate chamomile oil creams at graded concentrations and evaluate their performance against base cream and a betamethasone reference comparator where applicable. The study assessed formulation quality, stability, skin compatibility, in vitro release behavior, orthokeratosis-related antipsoriatic activity, histological improvement, and supportive docking and ADMET findings. The objective was to identify the most suitable stable chamomile oil cream formulation for further preclinical development as a potential topical candidate for psoriasis-related inflammatory skin changes.

## MATERIALS AND METHODS

This study was designed as an experimental preclinical formulation study to develop and evaluate chamomile essential oil-based oil-in-water topical cream formulations for psoriasis-related inflammatory skin changes. The study included chemical profiling of chamomile oil, preparation of topical cream formulations at graded concentrations, physicochemical characterization, accelerated stability testing, microbial evaluation, acute dermal irritation testing, in vitro release assessment using a modified Franz diffusion cell, antipsoriatic activity testing in a mouse-tail model, histopathological assessment, molecular docking, and ADMET prediction. The experimental workflow was structured to identify the most stable and biologically active chamomile oil cream formulation for further preclinical development.

*Table 1. Overall Experimental Workflow*

Experimental stage	Purpose	Main output
<b>GC-MS analysis of chamomile oil</b>	Chemical profiling of volatile and semi-volatile constituents	Identified compounds, retention time, base peak, molecular weight
<b>Formulation development</b>	Preparation of oil-in-water chamomile oil creams	C, C1, C2, C3, and C4 formulations
<b>Physicochemical evaluation</b>	Assessment of topical suitability	Organoleptic properties, pH, viscosity, spreadability, bleeding, loss on drying
<b>Stability and microbial testing</b>	Assessment of storage behavior and visible contamination	Homogeneity, phase separation, appearance, microbial growth
<b>Acute dermal irritation testing</b>	Preliminary skin compatibility assessment	Erythema and edema scores
<b>Mouse-tail antipsoriatic activity</b>	Preclinical biological activity assessment	Orthokeratosis and drug activity
<b>Histopathology</b>	Microscopic confirmation of epidermal changes	Granular layer and epidermal morphology
<b>Franz diffusion testing</b>	Assessment of in vitro release behavior	Time-specific calculated release values
<b>Molecular docking</b>	Exploratory target–ligand interaction assessment	Predicted binding interactions and scores where available
<b>ADMET prediction</b>	In silico pharmacokinetic and toxicity screening	Absorption, metabolism, toxicity, lipophilicity, and physicochemical parameters

Chamomile essential oil was analyzed by gas chromatography–mass spectrometry using a Shimadzu QP-2010 mass spectrometer equipped with an HP-5 non-polar column. The oil sample was diluted in hexane before analysis. The GC-MS system was operated in electron ionization mode at 70 eV, and mass spectra were scanned over an  $m/z$  range of 35–500. The column temperature was initially maintained at 50°C and then gradually increased to 280°C with a holding period. The chromatographic and mass spectral data were processed using Shimadzu software, and compound identification was performed by comparing acquired spectra with entries in the NIST 14 mass spectral database. The identified compounds were recorded according to compound name, IUPAC name, base peak, retention time,

molecular weight, and molecular formula where available. Peak-area percentages and library match scores were not available in the manuscript dataset and were therefore not used for quantitative interpretation of the oil composition.

**Table 2. GC-MS Method Parameters Reported in the Manuscript**

Parameter	Reported method detail
<b>Instrument</b>	Shimadzu QP-2010 mass spectrometer
<b>Column</b>	HP-5 non-polar column
<b>Dilution solvent</b>	Hexane
<b>Ionization mode</b>	Electron ionization
<b>Ionization energy</b>	70 eV
<b>Mass scan range</b>	35–500 m/z
<b>Initial column temperature</b>	50°C
<b>Final column temperature</b>	280°C
<b>Compound identification</b>	Shimadzu software and NIST 14 database matching
<b>Quantitative limitation</b>	Peak-area percentages and library match scores were not provided

Oil-in-water cream formulations containing chamomile essential oil were prepared using a previously described base cream preparation method with modification for graded oil incorporation (10). The base formulation contained stearic acid 15 g, cetyl alcohol 0.5 g, EDTA 0.2 g, sodium hydroxide 0.18 g, potassium hydroxide 0.5 g, glycerin 6 g, methyl paraben 0.15 g, and distilled water in sufficient quantity to prepare 100 g of cream. The aqueous and oily phases were prepared separately. The aqueous phase was heated to 80°C, while the oily phase containing cetyl alcohol and stearic acid was heated to 75°C. The two phases were combined under continuous vigorous agitation to obtain the cream base. Chamomile essential oil was then incorporated into separate portions of the base to obtain formulations coded as C1, C2, C3, and C4, containing 1.25%, 2.5%, 5%, and 7.5% chamomile oil, respectively. The base formulation without chamomile oil was coded as C. Each prepared formulation was adjusted to a final weight of 100 g with distilled water and stored in suitable containers for subsequent evaluation.

**Table 3. Composition and Formulation Codes of Chamomile Oil Cream Preparations**

Formulation code	Chamomile oil concentration
<b>C</b>	0%
<b>C1</b>	1.25%
<b>C2</b>	2.5%
<b>C3</b>	5%
<b>C4</b>	7.5%

**Table 4. Base Cream Excipients Used for 100 g Formulation**

Excipient	Quantity
<b>Stearic acid</b>	15 g
<b>Cetyl alcohol</b>	0.5 g
<b>EDTA</b>	0.2 g
<b>Sodium hydroxide</b>	0.18 g
<b>Potassium hydroxide</b>	0.5 g
<b>Glycerin</b>	6 g
<b>Methyl paraben</b>	0.15 g
<b>Distilled water</b>	Quantity sufficient to 100 g

The prepared cream formulations were evaluated for organoleptic characteristics, including color, odor, texture, and general appearance. These characteristics were assessed visually and by touch to determine topical acceptability. The pH of each formulation was measured using a digital pH meter to assess compatibility with skin application. Viscosity was evaluated using a Brookfield viscometer with spindle number 6. The cream samples were placed in appropriate containers, the spindle was immersed in each formulation, and viscosity was measured at rotational speeds of 5, 10, 20, 50, and 100 rpm.

Spreadability was assessed by placing a small quantity of cream between two glass slides and applying a 25 g weight over the upper slide. Spreadability was calculated using the following formula:

$$\text{Spreadability} = (W \times L) / T$$

where W is the weight placed on the upper slide, L is the length travelled by the slide, and T is the time required for spreading.

Bleeding was evaluated by storing the formulations under refrigerated and room-temperature conditions and observing whether liquid separated from the cream matrix. Loss on drying was determined by placing 2 g of each cream formulation in a china dish and maintaining it in an oven at 105°C. Loss on drying was calculated using the following formula:

$$\text{Loss on drying (\%)} = [(W_i - W_f) / W_i] \times 100$$

where  $W_i$  is the initial weight of the cream sample and  $W_f$  is the final weight after drying.

**Table 5. Physicochemical Evaluation Parameters and Calculation Methods**

Parameter	Method summary	Equation or output
<b>Organoleptic properties</b>	Visual and tactile assessment	Color, odor, texture, appearance
<b>pH</b>	Digital pH meter	pH value
<b>Viscosity</b>	Brookfield viscometer, spindle no. 6, 5–100 rpm	Viscosity in centipoise
<b>Spreadability</b>	Cream placed between two slides under 25 g weight	$\text{Spreadability} = (W \times L) / T$
<b>Bleeding</b>	Storage under refrigerated and room-temperature conditions	Presence or absence of liquid separation
<b>Loss on drying</b>	2 g cream heated at 105°C	$\text{Loss on drying (\%)} = [(W_i - W_f) / W_i] \times 100$

Accelerated stability testing was conducted in accordance with ICH-guided stability principles (11). The prepared cream formulations were packed in amber-colored jars and stored in a stability chamber at 40°C and 75% relative humidity for three months. Formulations were evaluated on days 0, 15, 30, and 90 for homogeneity, phase separation, ease of removal, texture, and appearance. Stability performance was compared across the different chamomile oil concentrations. Formulation C4 was assessed during the formulation and stability phase but was excluded from subsequent mouse-tail efficacy testing because it developed instability, phase separation, gritty texture, and small lumps during storage.

Microbial growth was assessed using the streak plate method. Agar medium was prepared, poured into Petri dishes, and allowed to solidify. Each cream formulation was applied to the medium, while a separate plate without cream served as the control. Plates were incubated at 37°C for 24 hours and then examined for visible microbial growth.

**Table 6. Stability and Microbial Evaluation Protocol**

Test	Conditions or method	Assessment time points	Main assessment criteria
<b>Accelerated stability</b>	Amber jars in stability chamber at 40°C and 75% relative humidity	Day 0, 15, 30, and 90	Homogeneity, phase separation, ease of removal, texture, appearance
<b>Microbial growth</b>	Streak plate method on agar medium	After 24 h incubation at 37°C	Visible microbial growth or absence of growth
<b>C4 decision</b>	Stability evaluation before efficacy testing	During storage assessment	Excluded from mouse-tail efficacy testing due to instability and phase separation

Acute dermal irritation testing was performed in accordance with OECD guideline 404 (12). The test was conducted in mice to maintain consistency with the animal model used for antipsoriatic activity assessment. The dorsal skin region was shaved before application of the prepared cream formulations. A limited quantity of the cream was applied to the shaved area and covered with a small gauze patch. The treated skin was examined one hour after application and then at 4, 24, and 48 hours for signs of

erythema and edema. Irritation responses were scored using a standard scale in which 0 indicated absence of erythema or edema and 4 indicated severe erythema or edema.

**Table 7. Erythema and Edema Scoring System for Acute Dermal Irritation**

Score	Erythema observation	Edema observation
0	No erythema	No edema
1	Very slight erythema	Very slight edema
2	Well-defined erythema	Slight edema
3	Moderate to severe erythema	Moderate edema
4	Severe erythema	Severe edema

For antipsoriatic activity assessment, healthy adult albino mice weighing 25–30 g were used. Animals were acclimatized before treatment and maintained in polypropylene cages under a 12-hour light–dark cycle at  $27 \pm 3^\circ\text{C}$  and  $52 \pm 3\%$  relative humidity. The mice were provided standard diet and drinking water ad libitum. A total of 18 mice were allocated into six groups, with three mice per group. The groups consisted of a betamethasone reference comparator group, a normal control group, a base cream control group, and chamomile oil cream treatment groups receiving C1, C2, and C3 formulations containing 1.25%, 2.5%, and 5% chamomile oil, respectively. Although C4 contained 7.5% chamomile oil and was prepared during the formulation phase, it was not included in the mouse-tail efficacy analysis because formulation instability and phase separation were observed during stability evaluation. All animal procedures were reported as being conducted according to recognized standard guidelines after ethical committee approval.

**Table 8. Animal Grouping for Mouse-Tail Antipsoriatic Activity Testing**

Group	Treatment	Formulation or comparator	Number of mice
Group I	Reference comparator	Betamethasone cream	3
Group II	Normal control	No active treatment	3
Group III	Base control	Base cream formulation C	3
Group IV	Chamomile oil cream	C1, 1.25% chamomile oil	3
Group V	Chamomile oil cream	C2, 2.5% chamomile oil	3
Group VI	Chamomile oil cream	C3, 5% chamomile oil	3
<b>Not included in efficacy testing</b>	Chamomile oil cream	C4, 7.5% chamomile oil	Excluded due to instability

The mouse-tail model was used to assess antipsoriatic activity through induction of orthokeratotic regions and evaluation of granular layer formation. A dose of approximately 2–5 mg of the assigned cream or comparator treatment was applied topically to the proximal region of the mouse tail once daily for two weeks. A plastic cylinder was fixed to the tail to maintain the formulation in contact with the treatment area for two hours. After the contact period, the remaining formulation was removed using a cotton ball. Animals were monitored during the study for clinical illness, abnormal behavior, body-weight change, and mortality.

Two hours after the final treatment application, mice were euthanized, and tail specimens were collected for histopathological evaluation. The tail samples were fixed in 10% buffered formalin, processed for sectioning, cut into 5  $\mu\text{m}$  sections, stained with hematoxylin and eosin, and permanently mounted on glass slides. The stained sections were examined under a light microscope. Histological assessment focused on epidermal morphology, granular layer formation, orthokeratotic regions, and scale-region measurements. For each tail sample, ten orthokeratosis measurements were recorded.

Percentage orthokeratosis was calculated using the following formula:

$$\text{Percentage orthokeratosis} = (A / B) \times 100$$

where A is the length of the granular layer and B is the total length of the scale region. Drug activity was calculated using the following formula: Drug activity (%) = [(Mean OK of treated group – Mean OK of control group) / (100 – Mean OK of control group)] × 100

where Mean OK of treated group is the mean percentage orthokeratosis in the treated group and Mean OK of control group is the mean percentage orthokeratosis in the control group.

**Table 9. Histological and Antipsoriatic Activity Outcomes**

Outcome	Definition or measurement	Calculation
<b>Granular layer length</b>	Length of granular layer in tail epidermal section	Direct histological measurement
<b>Scale-region length</b>	Total length of scale region in tail epidermal section	Direct histological measurement
<b>Orthokeratosis percentage</b>	Proportion of granular layer relative to scale region	Percentage orthokeratosis = (A / B) × 100
<b>Drug activity percentage</b>	Increase in orthokeratotic regions compared with control	Drug activity (%) = [(Mean OK treated – Mean OK control) / (100 – Mean OK control)] × 100
<b>Histological improvement</b>	Epidermal architecture and granular layer restoration	Qualitative microscopic assessment

In vitro release testing was performed for the selected optimized cream formulation using a modified Franz diffusion cell at the Pharmacy Institute, University of Veterinary & Animal Sciences, Lahore. The donor chamber contained the cream formulation, while the receptor chamber contained phosphate buffer solution. The receptor medium was maintained at 37°C with magnetic stirring at 50–100 rpm. Samples were withdrawn from the receptor chamber at 15, 30, 45, 60, 90, 120, and 150 minutes using a microsyringe, and the withdrawn volume was replaced with fresh phosphate buffer after each sampling point. Absorbance was measured using a UV spectrophotometer with phosphate buffer as the blank.

Concentration was calculated according to Beer–Lambert’s law using the following formula:  $A = a \times b \times c$ . Therefore:

$$c = A / (a \times b)$$

where A is absorbance, a is molar absorptivity, b is path length, and c is the calculated concentration.

The amount of drug released at each sampling time was calculated using the following formula:

$$\text{Amount released at time } t = V \times Ct$$

where V is the receptor medium volume and Ct is the calculated concentration at time t. Percentage release was calculated relative to the formulation-associated active constituent loaded in the donor compartment using the following formula: Release (%) = (Amount released at time t / Initial amount loaded) × 100. Because the available release data were reported as decreasing percentages over time, the values were treated as time-specific calculated release percentages rather than cumulative release unless further raw data confirm a cumulative-release calculation.

**Table 10. Franz Diffusion Cell Release-Testing Protocol**

Parameter	Reported detail
<b>Apparatus</b>	Modified Franz diffusion cell
<b>Site</b>	Pharmacy Institute, University of Veterinary & Animal Sciences, Lahore
<b>Donor chamber</b>	Cream formulation
<b>Receptor medium</b>	Phosphate buffer solution
<b>Temperature</b>	37°C
<b>Stirring speed</b>	50–100 rpm
<b>Sampling points</b>	15, 30, 45, 60, 90, 120, and 150 minutes
<b>Sample withdrawal</b>	Microsyringe

Parameter	Reported detail
Replacement	Fresh phosphate buffer after each withdrawal
Measurement	UV spectrophotometry
Blank	Phosphate buffer
Concentration equation	$c = A / (a \times b)$
Amount released	Amount released at time $t = V \times Ct$
Interpretation caution	Reported percentages decrease over time; therefore, they should not be labelled cumulative release unless recalculated from raw data

Molecular docking was performed to explore possible interactions between selected chamomile oil-associated ligands and protein targets relevant to psoriasis-related inflammatory pathways. The selected target proteins were tumor necrosis factor-alpha, aryl hydrocarbon receptor, phosphodiesterase 4D, Janus kinase 1, and interleukin-17 receptor A, represented by PDB IDs 2AZ5, 3QWR, 5K1I, 5TTS, and 7VKT, respectively. Protein–ligand complexes were obtained from the Protein Data Bank. Before docking, non-essential molecules, including co-crystallized water molecules and other non-relevant small molecules, were removed. Protein structures were protonated using the Protonate 3D function in MOE software and subjected to energy minimization. The native ligand was extracted from the binding site after protein preparation.

Eight ligand sets, including the lead ligand 2,2,2-trichloro-1-(2-nitrophenylthioamino)ethanol, were prepared in multiple conformations using the automated conformation search function in MOE. Molecular docking was performed using MOE Dock. Ligand placement was carried out using the Triangle Matcher algorithm, and binding poses were scored using the London dG scoring function, which estimates binding free energy using hydrogen bonding, ligand flexibility, rotational and translational entropy, and desolvation parameters (13). Docking validation was performed by re-docking the native co-crystallized ligand into the active site and selecting grid parameters that produced the lowest root mean square deviation.

**Table 11. Molecular Docking Targets and Docking Workflow**

Target protein	PDB ID	Relevance to psoriasis-related pathway	Docking preparation and scoring
<b>Tumor necrosis factor-alpha</b>	2AZ5	Central inflammatory cytokine	MOE preparation, Protonate 3D, energy minimization, Triangle Matcher, London dG
<b>Aryl hydrocarbon receptor</b>	3QWR	Immune and inflammatory signaling relevance	MOE preparation, Protonate 3D, energy minimization, Triangle Matcher, London dG
<b>Phosphodiesterase 4D</b>	5K1I	Inflammatory signaling modulation	MOE preparation, Protonate 3D, energy minimization, Triangle Matcher, London dG
<b>Janus kinase 1</b>	5TTS	Cytokine signaling pathway	MOE preparation, Protonate 3D, energy minimization, Triangle Matcher, London dG
<b>Interleukin-17 receptor A</b>	7VKT	IL-17 pathway involvement	MOE preparation, Protonate 3D, energy minimization, Triangle Matcher, London dG

ADMET analysis was conducted for the selected lead compound to predict pharmacokinetic and toxicity-related properties relevant to topical development. The assessed parameters included intestinal absorption, P-glycoprotein substrate status, volume of distribution, blood–brain barrier permeability expressed as logBB, cytochrome P450 substrate and inhibitor profile, total clearance, Ames toxicity prediction, synthetic accessibility, Lipinski drug-likeness, water solubility indices, lipophilicity values including consensus LogP, rotatable bonds, hydrogen-bond acceptors, hydrogen-bond donors, and topological polar surface area. The ADMET findings were interpreted as supportive in silico predictions and were not considered confirmatory evidence of safety or efficacy (15, 16).

Statistical analysis was performed using SPSS software. Available quantitative outcomes from the mouse-tail model were analyzed using one-way analysis of variance to compare treatment groups. Statistical significance was set at  $p < 0.05$ . Reported p-values were interpreted according to standard statistical reporting conventions, with values reported as exact p-values where available and values reported as 0.00 requiring correction to  $p < 0.001$  if supported by the original statistical output. The available manuscript did not specify normality testing, homogeneity-of-variance testing, post hoc comparison method,

confidence intervals, effect sizes, multiple-comparison adjustment, or missing-data handling; therefore, these analyses were not added beyond the reported ANOVA framework.

**Table 12. ADMET Parameters Assessed for the Selected Lead Compound**

ADMET domain	Parameters assessed
<b>Absorption</b>	Human intestinal absorption, P-glycoprotein substrate status
<b>Distribution</b>	Volume of distribution, blood–brain barrier permeability/logBB
<b>Metabolism</b>	CYP substrate and inhibitor profile, including CYP2D6, CYP3A4, CYP1A2, CYP2C19, and CYP2C9
<b>Excretion</b>	Total clearance
<b>Toxicity</b>	Ames toxicity prediction
<b>Drug-likeness</b>	Lipinski rule assessment, synthetic accessibility
<b>Water solubility</b>	ESOL, Ali, and SILICOS-IT logS values
<b>Lipophilicity</b>	iLOGP, XLOGP3, WLOGP, MLOGP, SILICOS-IT, consensus LogP
<b>Physicochemical properties</b>	Rotatable bonds, hydrogen-bond acceptors, hydrogen-bond donors, TPSA

**Table 13. Statistical Analysis Plan Based on Available Manuscript Information**

Analysis component	Reported or applied approach
<b>Software</b>	SPSS software
<b>Main inferential test</b>	One-way analysis of variance
<b>Significance threshold</b>	$p < 0.05$
<b>Main outcomes analyzed</b>	Orthokeratotic regions and granular layer length
<b>P-value reporting rule</b>	Exact p-values where available; $p = 0.00$ should be corrected to $p < 0.001$ if supported by output
<b>Not reported in manuscript</b>	SPSS version, normality testing, homogeneity-of-variance testing, post hoc test, confidence intervals, effect sizes, multiple-comparison correction, missing-data handling

## RESULTS

GC-MS analysis of chamomile essential oil identified several annotated volatile and semi-volatile compounds. The identified compounds included alpha-pinene, isodurene, pinene, lupenyl acetate, 1,4-dithiane-1-oxide, a nitrofen-related annotation reported as 2,2,2-trichloro-1-(2-nitrophenylthioamino) ethanol, di-n-octyl phthalate, and DEHP. The chromatographic details, including base peak, retention time, and molecular weight, are summarized in Table 1. Representative chemical structures of the annotated compounds are shown in Figure 1. Because peak-area percentages and library match scores were not available, the GC-MS findings were interpreted qualitatively rather than as a quantitative chemical composition profile. Duplicate or similar retention times and base peaks were retained as reported but require verification from the original chromatogram before final submission.

**Table 1. GC-MS-Identified Compounds in Chamomile Oil**

Compound name	IUPAC name / database annotation	Base peak	Retention time	Molecular weight	Comment
<b>Alpha-pinene</b>	2,6,6-trimethylbicyclo[3.1.1]hept-2-ene	93.05	5.123	136	Peak area percentage not reported
<b>Isodurene</b>	Tricyclo[2.2.1.0(2,6)]heptane, 1,3,3-trimethyl	93.05	5.123	136	Same retention time/base peak as alpha-pinene; requires verification
<b>Pinene</b>	2,6,6-trimethylbicyclo[3.1.1]hept-2-ene	93.05	5.123	136	Duplicate/similar annotation; requires verification
<b>Lupenyl acetate</b>	3,21-dihydroxylup-20(29)-en-28-yl acetate	43.95	5.293	500	Peak area percentage not reported
<b>1,4-Dithiane-1-oxide</b>	1,4-Dithiane-1-oxide	43.95	5.293	136	Same retention time/base peak as other entries; requires verification
<b>Nitrofen-related annotation</b>	2,2,2-trichloro-1-(2-nitrophenylthioamino) ethanol	43.95	5.293	316	Reported as lead docking compound; identity should be verified
<b>Di-n-octyl phthalate</b>	Di-n-octyl phthalate	29.123	148.9	390	Retention time appears unusual; verify chromatogram output
<b>DEHP</b>	Bis(2-ethylhexyl) phthalate	29.123	148.9	390	Possible phthalate/plasticizer annotation; verify source and contamination possibility

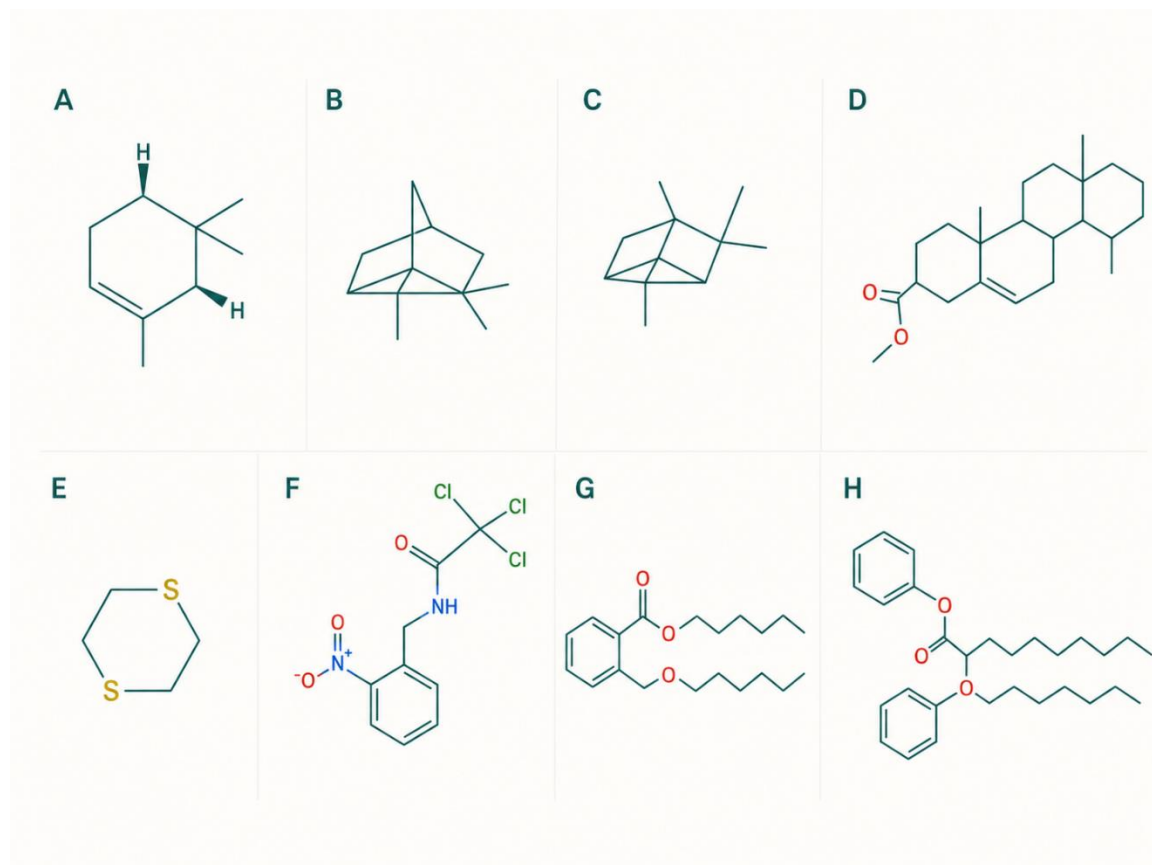


**Figure 1. Representative Chemical Structures of GC-MS-Identified Compounds in Chamomile Oil.** Representative chemical structures of compounds annotated in chamomile oil by GC-MS analysis. Compound identification was based on comparison of acquired mass spectra with the NIST 14 database. The structures are presented as qualitative visual annotations only because peak-area percentages and library match scores were not reported.

Chamomile oil was successfully incorporated into oil-in-water cream formulations at concentrations of 1.25%, 2.5%, 5%, and 7.5%, coded as C1, C2, C3, and C4, respectively. The base cream without chamomile oil was coded as C. C1, C2, and C3 retained smooth texture and acceptable appearance, whereas C4 showed small lumps and a gritty texture during organoleptic evaluation. The color intensity and odor increased progressively with increasing chamomile oil concentration, indicating concentration-dependent changes in formulation appearance and sensory characteristics.

**Table 2. Formulation Codes and Description of Chamomile Oil Cream Preparations**

Formulation code	Chamomile oil concentration	Formulation description	Use in study
C	0%	Base cream without chamomile oil	Used as base/control formulation
C1	1.25%	Chamomile oil oil-in-water cream	Evaluated for physicochemical, stability, irritation, and mouse-tail activity
C2	2.5%	Chamomile oil oil-in-water cream	Evaluated for physicochemical, stability, irritation, and mouse-tail activity
C3	5%	Chamomile oil oil-in-water cream	Evaluated for physicochemical, stability, irritation, mouse-tail activity, and in vitro release
C4	7.5%	Chamomile oil oil-in-water cream	Evaluated for formulation/stability parameters but excluded from mouse-tail efficacy testing because of instability and phase separation

**Table 3. Organoleptic Properties of Chamomile Oil Cream Formulations**

Parameter	C1	C2	C3	C4	C
Color	Very light blue	Light blue	Moderate blue	Blue	Creamy white
Odor	Slight pungent	Characteristic pungent	Strong characteristic apple-like odor	Very strong apple-like odor	No odor
Texture	Smooth	Smooth	Smooth	Small lumps and gritty	Smooth

Physicochemical Evaluation of Chamomile Oil Cream Formulations

Table 4. Physicochemical Parameters of Chamomile Oil Cream Formulations

Parameter	C1 / Conc. 1	C2 / Conc. 2	C3 / Conc. 3	C4 / Conc. 4
pH	6.14	5.84	6.04	6.97
Viscosity at 5 rpm	26400	32600	27600	30600
Viscosity at 10 rpm	16400	21700	19200	19500
Viscosity at 20 rpm	14600	13800	12600	38200
Viscosity at 50 rpm	5530	5530	6300	5890
Viscosity at 100 rpm	3040	3250	3040	4200
Spreadability at 20 s	7.50	7.50	7.50	7.50
Spreadability at 16.6 s	9.00	9.00	9.00	9.00
Spreadability at 21.4 s	7.00	7.00	7.00	7.00
Spreadability at 10 s	15.00	15.00	15.00	15.00
Bleeding test	0.00	0.00	0.00	1.00
Loss on drying	8.50	8.00	9.50	14.80

Note: Viscosity values are reported as shown in the original figure; units should be confirmed as centipoise. Bleeding test appears coded as 0 = no bleeding and 1 = bleeding.

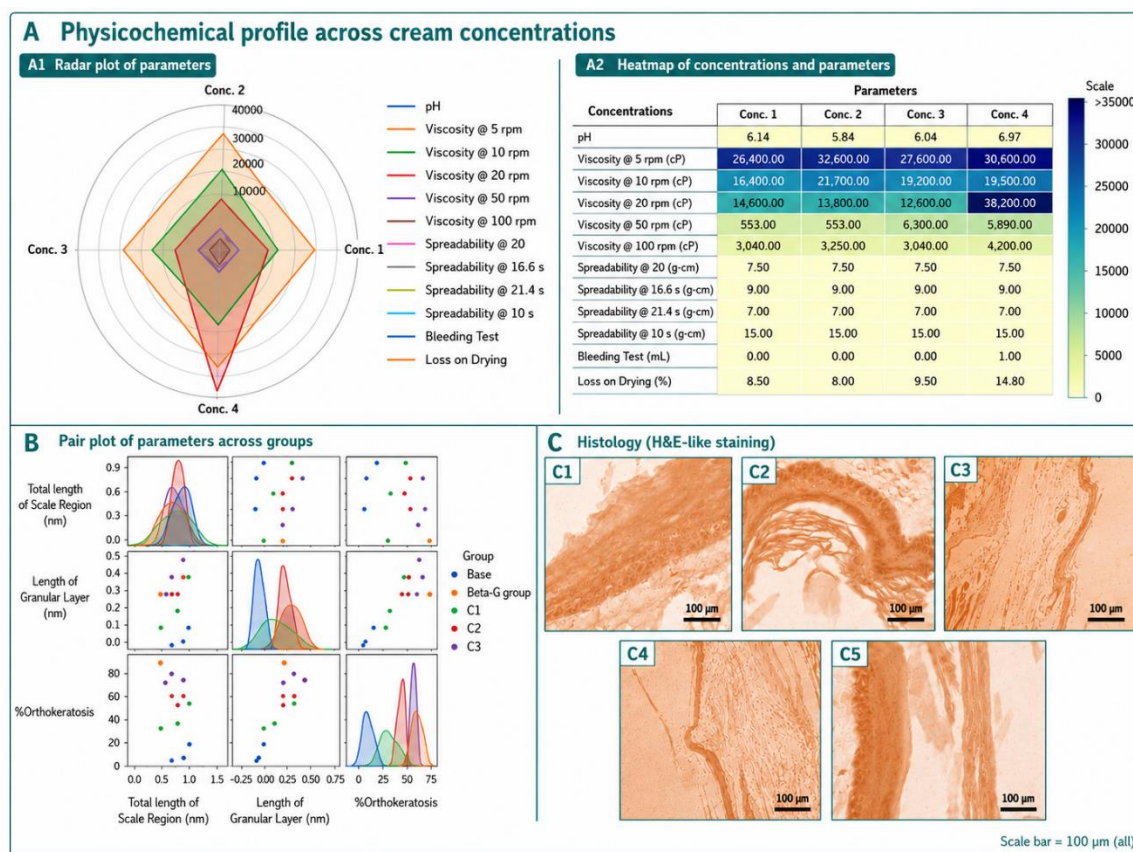


Figure 2. Physicochemical Profile of Chamomile Oil Cream Formulations. Multi-panel representation of physicochemical findings. Panel A shows the radar plot and heatmap of pH, viscosity, spreadability, bleeding test, and loss on drying across chamomile oil cream concentrations. Panel B shows the pairwise distribution of mouse-tail histological parameters across treatment groups. Panel C shows H&E-like histological images of mouse-tail epidermis across experimental groups. The figure uses teal-based visual formatting for clarity and should be interpreted alongside the numerical values reported in Tables 4, 8, and 9.

The physicochemical evaluation showed that C1, C2, and C3 had acceptable formulation characteristics for topical application. The pH values of C1, C2, and C3 were 6.14, 5.84, and 6.04, respectively, while C4 showed a higher pH of 6.97. Viscosity varied with rotational speed across all formulations, consistent with semisolid cream behavior. At 5 rpm, viscosity values were 26,400 for C1, 32,600 for C2, 27,600 for C3, and 30,600 for C4. At 100 rpm, the corresponding values decreased to 3,040, 3,250, 3,040, and 4,200, respectively. Spreadability values were similar across formulations at the assessed time points. The bleeding test was negative for C1, C2, and C3 but positive for C4. Loss on drying was 8.50 for C1, 8.00

for C2, 9.50 for C3, and 14.80 for C4, indicating a less favorable profile for the 7.5% formulation. These findings are summarized in Table 4 and visually presented in Figure 2.

Accelerated stability testing showed that C1, C2, and C3 remained stable throughout the observation period, with maintained homogeneity, absence of phase separation, and acceptable appearance. In contrast, C4 showed progressive instability. Although C4 was homogeneous initially, instability became evident during storage, with non-homogeneity and phase separation by day 30 and gritty texture with small lumps by day 90. Therefore, C4 was excluded from subsequent mouse-tail efficacy testing. No microbial growth was reported for any cream fraction after 24 hours of incubation.

**Table 5. Stability and Microbial Growth Observations Across Formulations**

Formulation	Day 0	Day 15	Day 30	Day 90	Overall stability interpretation	Microbial growth after 24 h
<b>C1</b>	Homogeneous, smooth semisolid	Stable	Stable	Stable	Stable formulation	No growth reported
<b>C2</b>	Homogeneous, smooth semisolid	Stable	Stable	Stable	Stable formulation	No growth reported
<b>C3</b>	Homogeneous, smooth semisolid	Stable	Stable	Stable	Stable formulation	No growth reported
<b>C4</b>	Homogeneous initially	Stability began to decline	Non-homogeneous with phase separation	Gritty, small lumps, unstable	Unstable formulation; excluded from efficacy testing	No growth reported

**Table 6. Binary Stability Coding Used in Stability Figure**

Formulation	Homogeneity Day 0	Homogeneity Day 15	Homogeneity Day 30	Homogeneity Day 90	Phase separation Day 0	Phase separation Day 15	Phase separation Day 30	Phase separation Day 90	Appearance Day 0	Appearance Day 15	Appearance Day 30	Appearance Day 90
<b>C1</b>	1	1	1	1	1	1	1	1	1	1	1	1
<b>C2</b>	1	1	1	1	1	1	1	1	1	1	1	1
<b>C3</b>	1	1	1	1	1	1	1	1	1	1	1	1
<b>C4</b>	1	1	0	0	1	1	0	0	1	0	0	0

Note: Coding follows the figure pattern: 1 = acceptable/homogeneous/no phase separation/smooth semisolid appearance; 0 = unacceptable/non-homogeneous/phase separation/other appearance. The exact coding labels should be verified before final submission.

The acute dermal irritation test showed no visible erythema or edema after topical application of the cream formulations according to the scoring system used in the study. In the mouse-tail model, topical application of chamomile oil cream formulations produced a concentration-associated increase in antipsoriatic activity among the stable formulations. Drug activity was 29.15% for C1, 44.90% for C2, and 61.12% for C3. The betamethasone reference comparator showed 66.38% drug activity. Thus, the 5% chamomile oil formulation showed the highest drug activity among the stable chamomile oil creams and approached the betamethasone comparator numerically. However, statistical equivalence with betamethasone was not established.

The pairwise distribution of total scale-region length, granular layer length, and percentage orthokeratosis showed a concentration-associated shift from C1 to C3, with C3 showing a distribution closer to the betamethasone-treated group than to the base control group. Histological examination further supported improvement in epidermal differentiation in treated groups, with more evident granular layer formation in the 5% chamomile oil cream group compared with the base control and lower-concentration formulations. These findings are visually summarized in Figure 2.

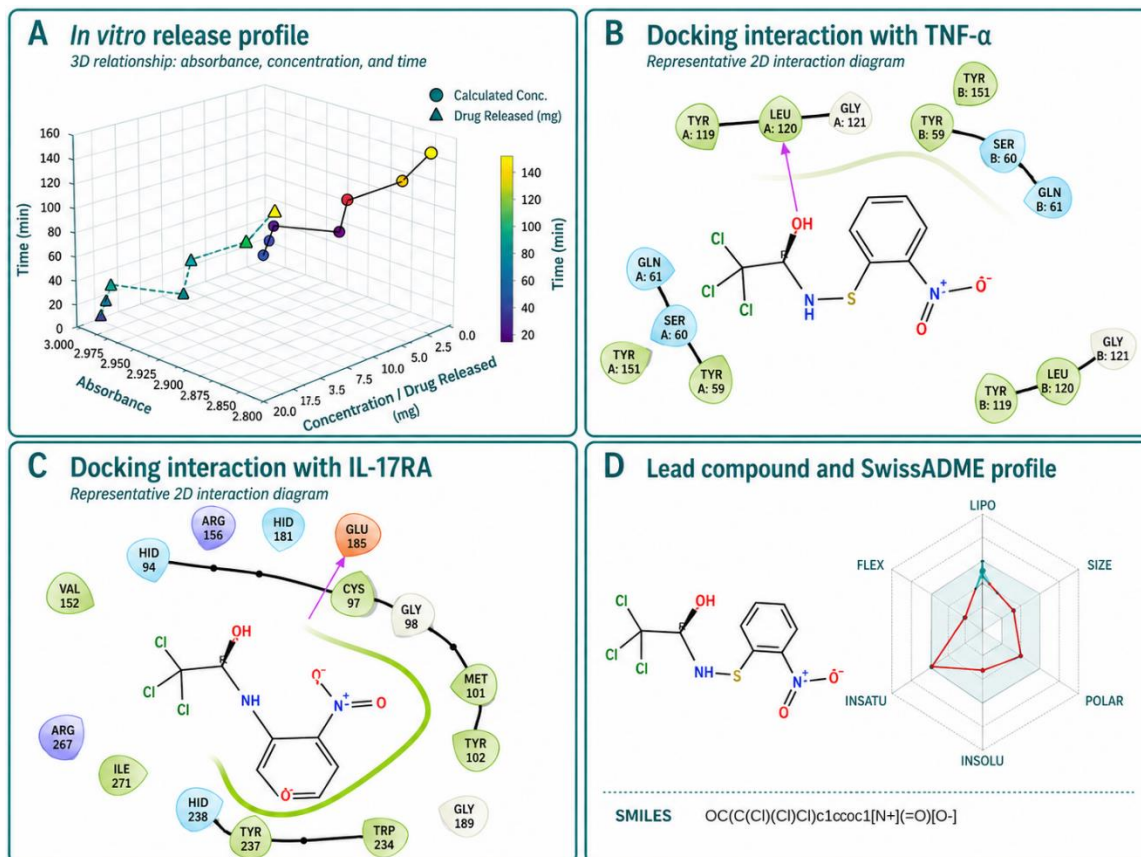


Figure 3. Stability Behavior of Chamomile Oil Cream Formulations. Stability profile of chamomile oil cream formulations during storage. C1, C2, and C3 maintained acceptable composite stability scores over the observation period, whereas C4 declined from acceptable status to instability, supporting its exclusion from mouse-tail efficacy testing.

Table 7. Acute Dermal Irritation Scoring System

Score	Erythema observation	Edema observation
0	No erythema	No edema
1	Very slight erythema	Very slight edema
2	Well-defined erythema	Slight edema
3	Moderate to severe erythema	Moderate edema
4	Severe erythema	Severe edema

Table 8. Mouse-Tail Antipsoriatic Activity: Drug Activity by Treatment Group

Treatment group	Formulation / comparator	Chamomile oil concentration	Drug activity (%)
C1	Chamomile oil cream	1.25%	29.15
C2	Chamomile oil cream	2.5%	44.90
C3	Chamomile oil cream	5%	61.12
Betamethasone	Reference comparator	Not applicable	66.38

Note: C3 showed the highest drug activity among the stable chamomile oil formulations. Betamethasone showed numerically higher activity than C3. Statistical equivalence between C3 and betamethasone was not established.

Table 9. Mouse-Tail Model: Reported Statistical Findings

Outcome	Statistical test	Reported p-value	Correct reporting format	Interpretation
Orthokeratotic regions	One-way ANOVA	0.00	p < 0.001, if confirmed by original SPSS output	Significant group difference reported
Granular layer length	One-way ANOVA	0.006	p = 0.006	Significant group difference reported
C1 versus base cream	Not fully specified	Not significant	Exact p-value not reported	No significant difference reported
Post hoc comparisons	Not reported	Not reported	Not reported	Requires original SPSS output

Note: p = 0.00 should not be reported in the final manuscript. It should be corrected to p < 0.001 only if supported by the original statistical output.

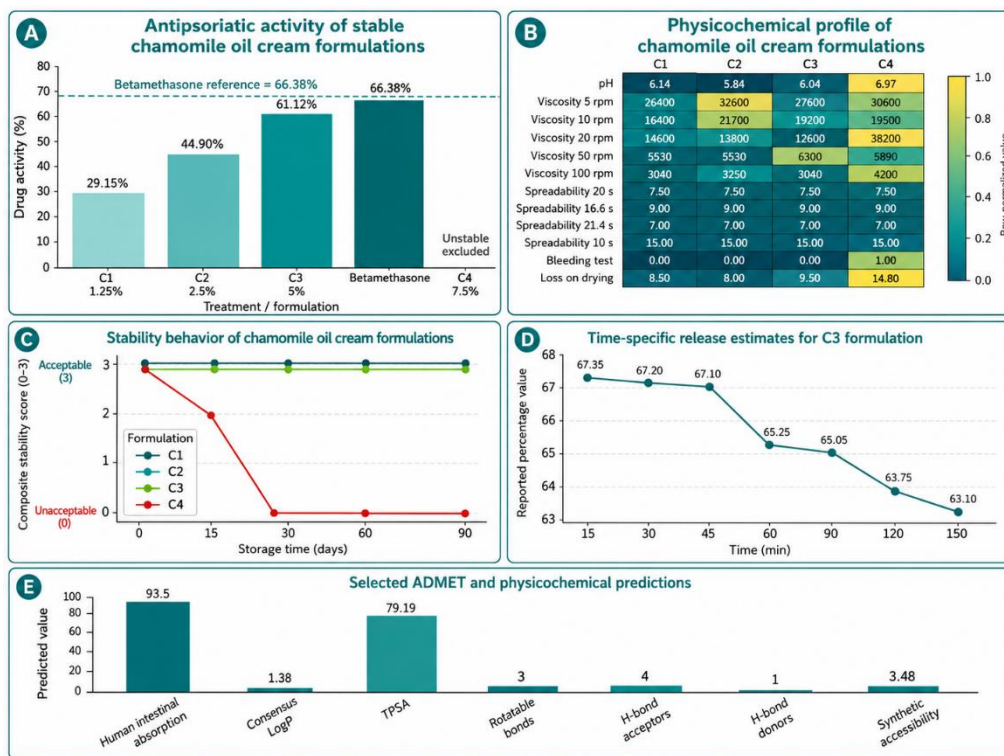


**Figure 4. Antipsoriatic Activity, Physicochemical Properties, Stability, Release, and ADMET Summary of Chamomile Oil Cream Formulations.** Multi-panel summary of key formulation and preclinical findings. Panel A shows antipsoriatic activity of stable chamomile oil cream formulations compared with the betamethasone reference comparator. Panel B shows row-normalized physicochemical properties across C1–C4. Panel C shows composite stability behavior over storage time, highlighting instability of C4. Panel D shows time-specific release estimates for the selected C3 formulation. Panel E shows selected ADMET and physicochemical predictions for the lead compound. Values are descriptive and should be interpreted with the limitations of available data.

The in vitro release assessment was conducted for the selected C3 formulation using a modified Franz diffusion cell. Reported percentage values were recorded at 15, 30, 45, 60, 90, 120, and 150 minutes. The reported percentage value was 67.35 at 15 minutes, 67.20 at 30 minutes, 67.10 at 45 minutes, 65.25 at 60 minutes, 65.05 at 90 minutes, 63.75 at 120 minutes, and 63.10 at 150 minutes. Because these values decreased over time, they should be interpreted as time-specific calculated release estimates rather than cumulative release unless recalculation from raw absorbance, concentration, receptor volume, replacement volume, and initial loading data confirms cumulative release. The release pattern is summarized in Tables 10 and 11 and visualized in Figures 4 and 5.

**Table 10. In Vitro Release Values of Selected C3 Chamomile Oil Cream Formulation**

Time point (min)	Reported percentage value
15	67.35
30	67.20
45	67.10
60	65.25
90	65.05
120	63.75
150	63.10

**Table 11. Interpretation of In Vitro Release Pattern**

Feature observed	Result	Interpretation caution
Time points assessed	15–150 min	Suitable for short-duration release observation
Percentage trend	Decreased from 67.35% to 63.10%	Not consistent with conventional cumulative release
Measurement basis	Absorbance and Beer–Lambert calculation	Calibration curve and wavelength not reported
Release terminology	Previously described as sustained release	Should be revised unless cumulative release is verified
Recommended wording	Time-specific calculated release estimates	Safer than “sustained” or “cumulative” release

**Figure 5. In Vitro Release, Docking Interactions, and SwissADME Profile of the Lead Compound.** Multi-panel representation of in vitro release and in silico findings. Panel A shows the 3D relationship among absorbance, calculated concentration/drug release, and time for the selected C3 formulation. Panel B shows the predicted docking interaction of the lead compound with TNF- $\alpha$ . Panel C shows the predicted docking interaction with IL-17RA. Panel D shows the lead compound structure and SwissADME-style bioavailability radar. These in silico findings are supportive and hypothesis-generating and should not be interpreted as confirmatory evidence of biological inhibition or clinical efficacy.

Molecular docking analysis was performed against psoriasis-related inflammatory targets, including TNF- $\alpha$ , IL-17RA, PDE4D, JAK1, and AhR. Among the reported docking observations, 2,2,2-trichloro-1-(2-nitrophenylthioamino)ethanol was identified as the lead compound with the highest reported binding affinity against TNF- $\alpha$ , with a docking score of -6.205 kcal/mol. For TNF- $\alpha$ , the predicted interaction included hydrogen bonding involving the hydroxyl group and Leu A:120, with additional hydrophobic and van der Waals interactions involving Tyr A:119, Tyr B:151, and Gly A:121. For IL-17RA, the predicted interaction included hydrogen bonding with Glu 185 and hydrophobic or van der Waals interactions involving Ile 271, Val 152, Tyr 102, and Met 101, with additional reported pocket-stabilizing residues including Arg 156, HID 94, and Cys 97. Docking findings are summarized in Tables 12 and 13 and illustrated in Figure 5. The results should be interpreted as computational predictions only and not as proof of target inhibition.

**Table 12. Molecular Docking Targets and Reported Top-Ligand Findings**

Target protein	PDB ID	Reported docking observation	Lead compound / ligand finding	Binding score
<b>Tumor necrosis factor-alpha</b>	2AZ5	Highest binding affinity among tested ligands reported for selected lead compound	2,2,2-trichloro-1-(2-nitrophenylthioamino)ethanol	-6.205 kcal/mol
<b>Interleukin-17 receptor A</b>	7VKT	One or more ligands showed lower free binding energy than co-crystallized inhibitor	Specific comparative score not fully reported	Not reported
<b>Phosphodiesterase 4D</b>	5K1I	Binding trend stated as pending/incomplete	Not fully reported	Not reported
<b>Janus kinase 1</b>	5TTS	Binding trend stated as pending/incomplete	Not fully reported	Not reported
<b>Aryl hydrocarbon receptor</b>	3QWR	Binding trend stated as pending/incomplete	Not fully reported	Not reported

Note: Rows containing “not reported” require completion from original docking output before final publication. Unavailable docking scores should not be fabricated.

**Table 13. Key Docking Interactions Reported for Selected Lead Compound**

Target	PDB ID	Key reported interaction	Residues involved	Interpretation
<b>TNF-alpha</b>	2AZ5	Hydrogen bonding through hydroxyl group	Leu A:120	Predicted stabilizing interaction
<b>TNF-alpha</b>	2AZ5	Hydrophobic and van der Waals interactions	Tyr A:119, Tyr B:151, Gly A:121	Supports predicted binding in docking model
<b>IL-17RA</b>	7VKT	Hydrogen bonding through hydroxyl group	Glu 185	Predicted stabilizing interaction
<b>IL-17RA</b>	7VKT	Hydrophobic and van der Waals interactions	Ile 271, Val 152, Tyr 102, Met 101	Supports predicted binding in docking model
<b>IL-17RA</b>	7VKT	Additional pocket-stabilizing residues	Arg 156, HID 94, Cys 97	May contribute to ligand stability

Note: Docking interactions are computational predictions and should be interpreted as hypothesis-generating, not as proof of biological inhibition.

ADMET prediction was performed for the selected lead compound, C<sub>6</sub>H<sub>4</sub>Cl<sub>3</sub>NO<sub>4</sub>. The compound showed predicted human intestinal absorption of 93.5% and was not predicted to be a P-glycoprotein substrate. The predicted logBB value was -6.36, suggesting low blood–brain barrier permeability. The compound was not predicted as a CYP2D6 or CYP3A4 substrate, but it was predicted to inhibit CYP1A2 and CYP2C19. The compound satisfied Lipinski drug-likeness criteria and showed a synthetic accessibility score of 3.48. Lipophilicity estimates included iLOGP 1.35, XLOGP3 2.15, WLOGP 2.27, MLOGP 0.63, SILICOS-IT LogP 0.48, and consensus LogP 1.38. The compound had three rotatable bonds, four hydrogen-bond acceptors, one hydrogen-bond donor, and TPSA of 79.19 Å<sup>2</sup>. However, the positive Ames toxicity prediction represents a major safety caution and indicates the need for further toxicological validation before any therapeutic interpretation. ADMET findings are summarized in Tables 14 and 15 and visualized in Figures 4 and 5.

**Table 14. ADMET Profile of Selected Lead Compound**

Parameter domain	Parameter	Result
Compound formula	Compound	C <sub>6</sub> H <sub>4</sub> Cl <sub>3</sub> NO <sub>4</sub>
Absorption	Human intestinal absorption	93.5%
Absorption	P-glycoprotein substrate	No
Distribution	Volume of distribution	Not reported
Distribution	Blood-brain barrier permeability, logBB	-6.36
Metabolism	CYP2D6 substrate	No
Metabolism	CYP3A4 substrate	No
Metabolism	CYP1A2 inhibitor	Yes
Metabolism	CYP2C19 inhibitor	Yes
Metabolism	CYP2C9 inhibitor	No
Metabolism	CYP2D6 inhibitor	No
Metabolism	CYP3A4 inhibitor	No
Excretion	Total clearance	Not reported
Toxicity	Ames toxicity	Positive / Yes
Synthetic accessibility	Synthetic accessibility score	3.48
Drug-likeness	Lipinski rule	Yes
Water solubility	LogS ESOL	-2.88
Water solubility	LogS Ali	-3.45
Water solubility	LogS SILICOS-IT	-2.37
Lipophilicity	iLOGP	1.35
Lipophilicity	XLOGP3	2.15
Lipophilicity	WLOGP	2.27
Lipophilicity	MLOGP	0.63
Lipophilicity	SILICOS-IT LogP	0.48
Lipophilicity	Consensus LogP	1.38
Physicochemical properties	Rotatable bonds	3
Physicochemical properties	Hydrogen-bond acceptors	4
Physicochemical properties	Hydrogen-bond donors	1
Physicochemical properties	TPSA	79.19 Å <sup>2</sup>

**Table 15. ADMET Interpretation for Topical Development**

ADMET feature	Reported result	Relevance to topical development	Safety interpretation
Consensus LogP	1.38	Suggests balanced lipophilicity for skin partitioning	Potentially favorable for topical screening
TPSA	79.19 Å <sup>2</sup>	Compatible with passive diffusion considerations	Requires experimental confirmation
Rotatable bonds	3	Indicates limited molecular flexibility	May support permeability prediction
logBB	-6.36	Low predicted brain penetration	Suggests low CNS exposure if systemic absorption occurs
CYP1A2 inhibition	Yes	Potential interaction risk if systemic exposure occurs	Requires caution
CYP2C19 inhibition	Yes	Potential interaction risk if systemic exposure occurs	Requires caution
Ames toxicity	Positive	Indicates predicted mutagenicity risk	Major limitation; requires toxicological validation
Lipinski drug-likeness	Yes	Supports drug-like physicochemical profile	Does not establish safety or efficacy

Overall, the results indicate that chamomile oil could be incorporated into stable oil-in-water cream formulations up to 5%, with C3 showing the most favorable balance of formulation stability and preclinical antipsoriatic activity among the tested chamomile oil creams. C4 was not suitable for efficacy testing because of instability and phase separation. The mouse-tail findings suggested concentration-associated improvement in drug activity, with C3 approaching the betamethasone comparator numerically. However, incomplete statistical reporting, unclear cumulative-release interpretation, qualitative GC-MS data, incomplete docking outputs, and the positive Ames prediction require cautious interpretation.

## DISCUSSION

The present study developed and evaluated chamomile oil-based oil-in-water topical cream formulations using an integrated preclinical workflow that included GC-MS profiling, physicochemical characterization, stability testing, microbial assessment, acute dermal irritation evaluation, in vitro release testing, mouse-tail antipsoriatic activity, histological examination, molecular docking, and ADMET prediction. Among the tested formulations, the 5% chamomile oil cream formulation, coded C3, showed the most favorable overall profile among the stable formulations. It retained acceptable organoleptic and physicochemical characteristics, remained stable during the observation period, showed no reported microbial growth, produced the highest drug activity among the chamomile oil

formulations, and demonstrated histological evidence of improved epidermal differentiation in the mouse-tail model. The 7.5% formulation, coded C4, was not suitable for efficacy testing because it developed instability, phase separation, gritty texture, and small lumps during storage. This finding suggests that increasing chamomile oil concentration beyond 5% may compromise formulation acceptability and physical stability, even if higher concentrations might theoretically increase active-constituent loading.

The formulation findings are important because the therapeutic usefulness of a topical herbal preparation depends not only on the biological activity of its active constituents but also on its ability to remain stable, homogeneous, skin-compatible, and acceptable for application. The stable formulations, C1, C2, and C3, showed smooth texture and acceptable appearance, whereas C4 showed bleeding and higher loss on drying, followed by instability during storage. The pH values of C1, C2, and C3 were within a range generally compatible with topical application, while viscosity varied across rotational speeds, reflecting the semisolid nature of the cream system. These results indicate that chamomile oil can be incorporated into an oil-in-water cream base at concentrations up to 5% without the formulation instability observed at 7.5%. Therefore, the formulation data support C3 as the most appropriate candidate for further preclinical optimization rather than C4, despite the higher oil concentration of the latter.

The mouse-tail model findings showed a concentration-associated increase in antipsoriatic activity among the stable chamomile oil cream formulations. Drug activity increased from 29.15% with C1 to 44.90% with C2 and 61.12% with C3, while the betamethasone reference comparator showed 66.38% activity. This pattern suggests that increasing chamomile oil concentration within the stable formulation range improved orthokeratosis-related outcomes in the mouse-tail model. The C3 formulation numerically approached the betamethasone comparator, but this should not be interpreted as therapeutic equivalence because equivalence, non-inferiority, or superiority testing was not reported. The absence of complete post hoc comparisons, confidence intervals, and effect-size estimates also limits the strength of direct between-group conclusions. Therefore, the most appropriate interpretation is that the 5% chamomile oil formulation showed promising preclinical activity in this model and requires further validation.

Histological observations further supported the biological findings by showing improved epidermal architecture and more evident granular layer formation in treated groups, particularly in the C3 formulation. In the mouse-tail model, antipsoriatic activity is inferred from the ability of a treatment to promote orthokeratosis and granular layer formation, reflecting improved keratinocyte differentiation. The observed increase in percentage orthokeratosis and granular layer-related outcomes is therefore consistent with a potential keratinocyte-normalizing effect of the formulation. However, the mouse-tail model does not reproduce the full immunological, genetic, and systemic complexity of human psoriasis. For this reason, the findings should be considered preliminary preclinical evidence rather than proof of clinical efficacy in psoriasis patients.

The biological plausibility of chamomile oil in inflammatory skin conditions may be related to its reported phytochemical constituents and anti-inflammatory potential. The GC-MS analysis identified several annotated compounds, including alpha-pinene and other volatile or semi-volatile constituents. Chamomile oil is commonly associated with compounds such as  $\alpha$ -bisabolol, chamazulene, flavonoids, and terpene-related constituents, which have been linked with anti-inflammatory and antioxidant properties in dermatological contexts. In psoriasis, inflammatory pathways involving TNF- $\alpha$ , IL-17, IL-22, IFN- $\gamma$ , NF- $\kappa$ B-associated signaling, and keratinocyte hyperproliferation are central to disease expression. Therefore, a topical formulation containing chamomile oil may plausibly influence inflammatory and differentiation-related processes. Nevertheless, the GC-MS findings in this study were qualitative because peak-area percentages, library match scores, and chromatographic abundance values

were not reported. As a result, the chemical composition cannot be interpreted quantitatively, and the relative contribution of each identified compound to the observed biological activity remains uncertain.

The *in vitro* release findings require cautious interpretation. The reported percentage values for the selected C3 formulation decreased from 67.35% at 15 minutes to 63.10% at 150 minutes. This pattern is not consistent with conventional cumulative release, which would generally be expected to increase over time. Therefore, the release profile should not be described as cumulative release or sustained release unless the raw absorbance values, calibration equation, receptor volume, replacement correction, initial loading quantity, and cumulative-release calculations are verified. The safer interpretation is that the reported values represent time-specific calculated release estimates derived from absorbance and Beer–Lambert calculations. Future studies should clarify the wavelength, calibration curve, membrane type, receptor volume, diffusion area, sampling volume, replacement correction, sink conditions, and cumulative release calculation method before making claims about release kinetics.

The molecular docking results provide supportive mechanistic hypotheses but do not establish biological inhibition. The selected lead compound, 2,2,2-trichloro-1-(2-nitrophenylthioamino)ethanol, showed a reported docking score of -6.205 kcal/mol against TNF- $\alpha$  and predicted interactions involving Leu A:120, Tyr A:119, Tyr B:151, and Gly A:121. Additional docking interactions were reported for IL-17RA, including hydrogen bonding with Glu 185 and interactions with Ile 271, Val 152, Tyr 102, Met 101, Arg 156, HID 94, and Cys 97. These findings are compatible with possible interaction of the lead compound with psoriasis-relevant inflammatory targets, but docking is a computational screening method and cannot confirm receptor inhibition, pathway modulation, cellular activity, or *in vivo* pharmacodynamic effect. In addition, docking data were incomplete for PDE4D, JAK1, and AhR, and several binding scores were not reported. Therefore, the docking results should be framed as hypothesis-generating evidence that may guide future molecular or cellular validation.

The ADMET findings also require a balanced interpretation. The selected lead compound showed predicted human intestinal absorption of 93.5%, consensus LogP of 1.38, TPSA of 79.19 Å<sup>2</sup>, three rotatable bonds, four hydrogen-bond acceptors, and one hydrogen-bond donor. These physicochemical properties may be compatible with preliminary topical-delivery screening, but they do not establish dermal permeability, local retention, systemic safety, or therapeutic utility. The low predicted logBB value suggests limited brain penetration if systemic exposure occurs, but this does not remove other systemic risks. Predicted inhibition of CYP1A2 and CYP2C19 may indicate potential interaction concerns if the compound reaches systemic circulation, particularly with repeated or large-area topical application. Most importantly, the positive Ames toxicity prediction is a major safety caution. This finding should prevent any strong claim that the lead compound or formulation is definitively safe. Further experimental toxicology, including dermal toxicity, sensitization, repeated-dose safety, genotoxicity, and systemic exposure studies, is required before therapeutic translation.

The acute dermal irritation findings suggested absence of visible erythema and edema under the conditions tested, but this should be interpreted as limited local tolerability rather than comprehensive safety. The study did not report extended dermal toxicity, repeated-dose irritation scoring beyond the acute observation framework, sensitization testing, systemic biochemical safety markers, organ histology, or long-term exposure outcomes. Therefore, the phrase “non-irritant under the tested conditions” is more appropriate than “safe.” Similarly, the animal findings support preclinical antipsoriatic potential but not clinical effectiveness. The distinction between local irritation, systemic toxicity, mutagenicity prediction, and clinical safety should be clearly maintained.

Several limitations should be acknowledged. The study used a small number of animals per group, and no sample size rationale was reported. Details of randomization, allocation concealment, blinded histological assessment, animal sex, strain/source, and ethical approval number were incomplete. GC-MS reporting lacked peak-area percentages, library match scores, and verification of duplicate or unusual retention-time annotations. The *in vitro* release method lacked sufficient information to

confirm cumulative-release behavior. Statistical reporting was incomplete, with limited post hoc information, no confidence intervals, and no effect sizes. Docking results were incomplete for several targets, and ADMET predictions were not experimentally validated. The mouse-tail model is useful for screening orthokeratosis and keratinocyte differentiation, but it cannot fully model human plaque psoriasis. These limitations mean that the findings should be interpreted as early preclinical evidence supporting further investigation rather than definitive proof of efficacy or safety.

Future studies should optimize the 5% chamomile oil cream formulation through replicated physicochemical and stability testing, improved release-method validation, complete GC-MS quantification, and standardized skin permeation studies. The in vitro release profile should be recalculated using validated cumulative-release equations and appropriate replacement-volume correction. Larger animal studies should include clear randomization, blinded histological assessment, predefined primary outcomes, adequate sample size calculation, and complete statistical reporting. Additional toxicological assessment is particularly important because of the positive Ames prediction for the selected lead compound. Molecular docking findings should be followed by enzyme, receptor-binding, cell-based inflammatory-pathway, or cytokine-expression assays to determine whether the predicted interactions translate into biological activity. Only after robust preclinical validation should clinical studies be considered.

## CONCLUSION

The present preclinical study showed that chamomile oil could be incorporated into oil-in-water topical cream formulations, with the 5% formulation demonstrating the most favorable balance of stability, physicochemical acceptability, and mouse-tail antipsoriatic activity among the stable tested formulations. The 5% cream showed 61.12% drug activity, numerically approaching the betamethasone comparator value of 66.38%, while the 7.5% formulation was excluded from efficacy testing because of instability and phase separation. Histological findings supported improved epidermal differentiation and granular layer formation in the treated groups, particularly with the 5% formulation. The in vitro release findings should be interpreted cautiously as time-specific calculated release estimates rather than confirmed cumulative or sustained release. Docking and ADMET analyses provided supportive, hypothesis-generating information, but the positive Ames prediction represents an important safety concern. Further formulation optimization, validated release and permeation testing, expanded toxicological evaluation, larger controlled animal studies, and clinical trials are required before chamomile oil cream can be recommended for therapeutic application in humans.

## REFERENCES

1. Yamazaki F. Psoriasis: comorbidities. *J Dermatol*. 2021;48(6):732-40.
2. Zhu B, Jing M, Yu Q, Ge X, Yuan F, Shi L. Treatments in psoriasis: from standard pharmacotherapy to nanotechnology therapy. *Adv Dermatol Allergol*. 2022;39(3):460-71.
3. Wu M, Dai C, Zeng F. Cellular mechanisms of psoriasis pathogenesis: a systematic review. *Clin Cosmet Investig Dermatol*. 2023;16:2503-15.
4. Sieminska I, Pieniawska M, Grzywa TM. The immunology of psoriasis: current concepts in pathogenesis. *Clin Rev Allergy Immunol*. 2024;66(2):164-91.
5. Stanojevic LP, Marjanovic-Balaban ZR, Kalaba VD, Stanojevic JS, Cvetkovic DJ. Chemical composition, antioxidant and antimicrobial activity of chamomile flowers essential oil (*Matricaria chamomilla* L.). *J Essent Oil-Bear Plants*. 2016;19(8):2017-28.
6. Lee SH, Heo Y, Kim YC. Effect of German chamomile oil application on alleviating atopic dermatitis-like immune alterations in mice. *J Vet Sci*. 2010;11(1):35-41.

7. Zhu Y, Zhou Y, Ma X, Duan Z, Xu H, Li Y, et al. Topical therapy in psoriasis: clinical benefits, advances in novel drug delivery strategies, and gene therapy regimen. *Pharmaceutics*. 2025;17(3):283.
8. Kumar M, Sharma A, Mahmood S, Thakur A, Mirza MA, Bhatia A. Franz diffusion cell and its implication in skin permeation studies. *J Dispers Sci Technol*. 2024;45(5):943-56.
9. Karamani C, Antoniadou IT, Dimou A, Andreou E, Kostakis G, Sideri A, et al. Optimization of psoriasis mouse models. *J Pharmacol Toxicol Methods*. 2021;108:107054.
10. Nguyen Thanh Tram NTT, Hoang Le Son HLS. Assessment of anti-psoriatic activity of *Cassia fistula* L. extract incorporated cream. 2015.
11. Ali MS, Alam MS, Alam N, Anwer T, Safhi MMA. Accelerated stability testing of a clobetasol propionate-loaded nanoemulsion as per ICH guidelines. *Sci Pharm*. 2013;81(4):1089.
12. Organisation for Economic Co-operation and Development. Test No. 404: Acute Dermal Irritation/Corrosion. Paris: OECD Publishing; 2015.
13. García-Díaz JM, Garibaldi-Ríos AF, Gallegos-Arreola MP, Gutiérrez-Gutiérrez F, Delgado-Saucedo JI, Martínez-Velázquez M, et al. Computational workflow for chemical compound analysis: from structure generation to molecular docking. 2026;94(1):9.
14. Alvarez-Coiradas E, Munteanu CR, Diaz-Saez L, Pazos A, Huber KV, Loza MI, et al. Discovery of novel immunopharmacological ligands targeting the IL-17 inflammatory pathway. 2020;89:107026.
15. van de Waterbeemd H, Gifford E. ADMET in silico modelling: towards prediction paradise? *Nat Rev Drug Discov*. 2003;2(3):192-204.
16. Sucharitha P, Reddy KR, Satyanarayana S, Garg T. Absorption, distribution, metabolism, excretion, and toxicity assessment of drugs using computational tools. In: *Computational approaches for novel therapeutic and diagnostic designing to mitigate SARS-CoV-2 infection*. Amsterdam: Elsevier; 2022. p. 335-55.
17. Raharja A, Mahil SK, Barker JN. Psoriasis: a brief overview. *Clin Med (Lond)*. 2021;21(3):170-3.
18. Gharakhani A, Hamedeyazdan S, Entezari-Maleki T, Ghavimi H. Chamomile: an adjunctive herbal remedy for rheumatoid arthritis treatment. *Adv Biosci Clin Med*. 2013;1(1):20-6.
19. Safayhi H, Sabieraj J, Sailer ER, Ammon HP. Chamazulene: an antioxidant-type inhibitor of leukotriene B<sub>4</sub> formation. *Planta Med*. 1994;60(5):410-3.
20. Dai YL, Li Y, Wang Q, Niu FJ, Li KW, Wang YY, et al. Chamomile: a review of its traditional uses, chemical constituents, pharmacological activities and quality control studies. *Molecules*. 2023;28(1):133.
21. Özbek H, Sever Yilmaz B. Anti-inflammatory and hypoglycemic activities of alpha-pinene. *Acta Pharm Sci*. 2017;55(4).
22. Rahimi K, Zalaghi M, Shehnizad EG, Salari G, Baghdezfoli F, Ebrahimifar A. The effects of alpha-pinene on inflammatory responses and oxidative stress in the formalin test. *Brain Res Bull*. 2023;203:110774.
23. Gabbanini S, Neba JN, Matera R, Valgimigli L. Photochemical and oxidative degradation of chamazulene contained in *Artemisia*, *Matricaria* and *Achillea* essential oils and setup of protection strategies. *Molecules*. 2024;29(11):2604.